Synthesis of Coupling Matrix for Diplexers Based on a Self-Adaptive Differential Evolution Algorithm

Bo Liu, *Senior Member, IEEE*, Hao Yang, and Michael J. Lancaster, *Senior Member, IEEE*

***Abstract*— Diplexer coupling matrix synthesis often involves both analytical methods and optimization techniques. At present, general purpose optimization algorithms are used, but they need strong supporting information (e.g., high-quality starting points and very narrow search ranges) from analytical methods, which is not available or too complex to be obtained in many cases. Aiming to obtain the desired coupling matrix with highly reduced supporting information to relieve the pressure of analytical methods, a new optimization algorithm, called self-adaptive differential evolution for coupling matrix synthesis (SADEC), is proposed. Considering the landscape characteristics of diplexer coupling matrix synthesis problems, a new self-adaptive multipopulation search framework and a self-adaptive algorithm parameter control strategy are proposed and organized in a particular way. The performance of SADEC is demonstrated by two all-resonator-based narrowband diplexers using large search ranges only with the requirement of matching the diplexer topology and no *ad hoc* analysis is included. Experiments and comparisons show the high performance of SADEC and clear advantages compared with the state-of-the-art global optimization methods. SADEC is also applicable to filter coupling matrix synthesis and is downloadable.**

***Index Terms*— Coupling matrix, coupling matrix synthesis, differential evolution (DE), diplexer.**

I. Introduction

THE coupling matrix model is often employed in modern filter and diplexer design [1]. Because of the direct connection between the coupling matrix and the geometric parameters of the physical design, the coupling matrix is a widely used tool to obtain the initial geometric design parameters before 3-D full-wave electromagnetic (EM) simulation-based design optimization. Bandler *et al.* [2] and Liu *et al.* [3] show that both the local optimization and global optimization-based EM simulation-driven design optimization methods can benefit from a good initial design for complex filters and diplexers. Therefore, the high-quality synthesis of a coupling matrix is essential.

Manuscript received July 4, 2017; revised September 19, 2017; accepted September 30, 2017. Date of publication January 3, 2018; date of current version February 5, 2018. This work was supported by the U.K. Engineering and Physical Science Research Council under Project EP/M016269/1. *(Corresponding author: Bo Liu.)*

B. Liu is with the School of Electrical, Electronic and System Engineering, University of Birmingham, Birmingham B15 2TT, U.K., and also with the School of Applied Science, Computing and Engineering, Wrexham Glyndwr University, Wrexham LL11 2AW, U.K. (e-mail: b.liu.3@bham.ac.uk; liubo168@gmail.com).

H. Yang and M. J. Lancaster are with the School of Electrical, Electronic and System Engineering, University of Birmingham, Birmingham B15 2TT, U.K. (e-mail: hxy297@student.bham.ac.uk; m.j.lancaster@bham.ac.uk).

Color versions of one or more of the figures in this paper are available online at http://ieeexplore.ieee.org.

Digital Object Identifier 10.1109/TMTT.2017.2772855

Coupling matrix synthesis methods can be mainly classified into three categories: analytical methods [4]–[6], optimization-based methods [7]–[9], and hybrid analytical and optimization methods [10], [11]. In analytical methods, the appropriate coupling coefficient and external quality factor values are analytically calculated based on the properties of the microwave device. They are theoretically sound and with guaranteed good results. Optimization-based methods, on the other hand, obtain the appropriate coupling matrix through a black-box optimization process. Except for the selection of cost functions [9], [12], [13], much less theoretical analysis is involved, providing the advantages of ease of use and being general.

However, as the complexity of the response and topology increases, especially for multiport devices, both kinds of methods face challenges: the analytical methods can become intricate and sometimes impossible to realize [14] and the optimization methods may have a low success rate even with fine tuning of the cost function and the search range [9], [15]. Traditional genetic algorithms or genetic algorithm-based memetic/hybrid algorithms and state-of-the-art global optimization algorithms (e.g., differential evolution (DE) [16] and particle swarm optimization (PSO) [17]) are tested in our pilot experiments. The success rate is low for various diplexer coupling matrix synthesis problems.

Therefore, the hybrid analytical and optimization-based methods are attracting much attention. In such methods, an optimization engine is employed, but the optimization problem is highly simplified based on analytical methods, such as a high-quality starting point [11], a well-organized synthesis process [10], or highly reduced search ranges [18]. Due to such strong supporting information, the optimization algorithm does not need to be strong. At present, the widely used methods are general purpose optimization methods, such as Nelder–Mead simplex method [19], sequential quadratic programming [20], and evolutionary algorithms (EAs), which are widely used in microwave engineering [21]–[24].

However, the main application area of hybrid analytical and optimization-based methods is filter synthesis. To the best of our knowledge, for more complex topologies, such as the all-resonator-based diplexer, which is a new and promising component in satellite communication systems, there are a few matured coupling matrix synthesis methods. When applying the above hybrid method for diplexer synthesis, it is not easy to obtain a good enough starting point or the search range is not narrow enough in many cases, causing optimization not to be successful [15]. Hence, developing a strong optimization mechanism for complex coupling matrix synthesis, which

0018-9480 © 2018 British Crown Copyright

can considerably relieve the pressure of the prior analytical analysis, is important to complement the state of the art for coupling matrix synthesis for multiport devices.

Aiming to fill this gap, an optimization method for coupling matrix synthesis for diplexers, called self-adaptive DE for coupling matrix synthesis (SADEC), is proposed. The main innovations include a new self-adaptive multipopulation search framework and a self-adaptive DE algorithm parameter control strategy. Both of them are designed to tackle the landscape characteristics of the targeted problem. SADEC aims as follows.

1) To obtain highly optimal solutions for diplexer coupling matrix synthesis with a high success rate.
2) Do not rely on good initial values, highly reduced search ranges, or other specific properties of the targeted design cases.

We believe that if these two goals are met, diplexer coupling matrix synthesis with weak, easy to obtain, or highly reduced supporting information from analytical methods is expected to be successful in most cases. General purpose optimization techniques (e.g., sequential quadratic programming and PSO), which show difficulty for the targeted problem, can therefore be replaced.

The remainder of this paper is organized as follows. Section II introduces the basic techniques, including a brief introduction of the coupling matrix method and the standard DE algorithm. Section III introduces the SADEC algorithm, including its main ideas, the design of the new algorithm framework and algorithmic components and parameter setting. Section IV demonstrates SADEC by two all-resonator-based diplexers. Large search ranges only with the requirement of matching the diplexer topology are used. Comparisons with standard DE and PSO are also provided. The concluding remarks are provided in Section V.

II. Basic Techniques

A. Coupling Matrix Method for Diplexer Design

The S-parameter design specifications of a diplexer can be calculated using the scaled external quality factors q_{ei} and the general matrix $[A]$ using the following equations [18]:

$$S_{11} = \pm\left(1 - \frac{2}{q_{e1}}[A]^{-1}_{1,1}\right)$$
$$S_{i1} = 2\frac{1}{\sqrt{q_{e1}q_{ei}}}[A]^{-1}_{i,1}, \quad i = 2, \ldots, n \tag{1}$$

where n is the number of ports. The general matrix $[A]$ can be expressed as

$$[A] = [q] + p[U] - j[m] \tag{2}$$

where $[q]$ is an $n \times n$ matrix with all entries zero, except for $q_{ii} = (1/q_{ei}), i = 1, 2, \ldots, n$ (i stands for the index of a resonator connected to an external port), $[U]$ is an $n \times n$ identity matrix, p is the complex lowpass frequency variable, and $[m]$ is the general normalized coupling matrix, which is what SADEC targets at.

B. Differential Evolution Algorithm

The DE algorithm [16] is the fundamentals of SADEC. DE is a population-based global optimization algorithm, which outperforms many EAs for continuous optimization problems [16] and is widely used in the EM design optimization domain. Nevertheless, DE is not the only choice, other popular EAs (e.g., PSO and evolution strategy) may also be improved following similar ideas in this paper.

DE is an iterative method. In each iteration, the mutation operator is first applied to generate a population of mutant vectors. A crossover operator is then applied to the mutant vectors to generate a new population. Finally, selection takes place and the corresponding candidate solutions from the old population and the new population compete to comprise the population for the next iteration.

In the tth iteration, the ith candidate solution in the population, P, can be represented as

$$x^i(t) = \left[x^i_1, x^i_2, \ldots, x^i_d\right] \tag{3}$$

where d is the number of design variables.

In DE, mutation is the main approach to explore the design space. There are a few different DE mutation strategies trading off the convergence speed and the population diversity in different manners. Arguably, the most widely used one is DE/rand/1 [16], which is as follows:

$$v^i(t+1) = x^{r_1}(t) + F \cdot (x^{r_2}(t) - x^{r_3}(t)) \tag{4}$$

where x^{r_1}, x^{r_2}, and x^{r_3} are three different solutions randomly selected from the current population, P. v^i is the ith mutant vector in the population after mutation. $F \in (0, 2]$ is a control parameter, called the scaling factor.

Crossover is then applied to the population of mutant vectors to produce the child population U, which works as follows.

1) Randomly select a variable index $j_{\text{rand}} \in \{1, \ldots, d\}$.
2) For each $j = 1$ to d, generate a uniformly distributed random number rand from $(0, 1)$ and set

$$u^i_j(t+1) = \begin{cases} v^i_j(t+1), & \text{if } (\text{rand} \le \text{CR}) | j = j_{\text{rand}} \\ x^i_j(t), & \text{otherwise} \end{cases} \tag{5}$$

where $\text{CR} \in [0, 1]$ is a constant called the crossover rate.

Following that, the selection operation decides on the population of the next iteration, which is often based on a one-to-one greedy selection between P and U. Considering a minimization problem, the selection operator is

$$x^i(t+1) = \begin{cases} u^i(t+1), & \text{if } f(u^i(t+1)) < f(x^i(t)) \\ x^i(t), & \text{otherwise.} \end{cases} \tag{6}$$

III. SADEC Algorithm

A. Challenges and Motivations

Aiming to propose a general method for diplexer coupling matrix synthesis, case-specific information is not included

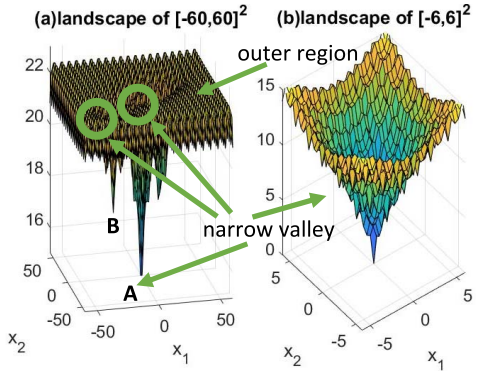

Fig. 1. Illustrative figure of diplexer coupling matrix synthesis problem landscape (the Ackley benchmark test function [25] is used for illustration).

in the cost function. Our cost function only involves violation of S-parameter constraints, such as $\max\{\max(|S_{11}|) - (-20 \text{ dB}), 0\}$ for the constraint of $\max|S_{11}| < -20$ dB in the passband(s). The cost function is defined as the sum of normalized S-parameter constraint violations. For normalization, the violation of each constraint for each candidate solution is divided by the maximum constraint violation so far for the corresponding constraint. Examples are shown in Section IV. Transmission and reflection zeros are not used due to generality consideration. Transmission zeros do not always exist. We also found that for some complex synthesis problems, there are many solutions with very close transmission and/or reflection zeros compared with the desired ones, but the S-parameter response is far away from the specifications.

Using the above cost function, by studying various diplexer coupling matrix synthesis problems (e.g., sampling and sweeping), Fig. 1 (illustrative figure) shows the characteristics of the landscape. It can be seen that: 1) if without an *ad hoc* selection of the search range, the optimal regions locate in several narrow valleys of the search space and the outer region is flat. This characteristic is understandable because most diplexers are narrowband, and resonance only happens in very particular design parameters; 2) the optimal regions are separated because these narrow valleys are not connected with each other; 3) the best solution in most of the narrow valleys is only a local optimum (point B in Fig. 1), which is not useful (an example is shown in Section IV-A); and 4) even in a narrow valley, the landscape is multimodal (has local optima).

EAs are stochastic optimization methods and there is always a balance between the exploration ability and the probability to find the correct search direction [26]. In a stochastic search process, if the diversity of possible movements is limited, it is easy to get trapped in a local optimum. When the diversity of possible movements increases, the capacity of exploring unknown space is promoted, but the probability to find the correct search direction decreases considerably. The characteristics of the targeted landscape require the optimization algorithm having a good exploration ability because it is multimodal. However, it also requires the algorithm having a high capacity to find the correct search direction because the optima locate in narrow valleys. In addition, most of the narrow valleys only provide local optima even if they are visited. Therefore, it is not a surprise that modern EAs, such as standard DE and PSO, have a very low success rate. Our pilot experiments show that standard DE and PSO have difficulty in converging at the global optimum and may converge at a local optimum (i.e., point B in Fig. 1).

In the computational intelligence field, various improved DE and PSO are proposed [27] and many of them focus on jumping out of local optima. Their general idea is to promote the exploration ability. However, these methods do not seem suitable for the targeted problem. These methods target at highly multimodal problems, but their optimal regions are not narrow and not separated [25]. Hence, finding the correct search direction is not a main consideration for those methods, but it is an important challenge for the coupling matrix synthesis problem. Arguably, the benchmark test problem with the narrowest optimal region used in the computational intelligence field is the Ackley function [25], while our experiments show that the optimal region of the targeted problem is much narrower than that of the Ackley function. Therefore, promoting exploration ability makes the optimization algorithm be trapped in the outer region when synthesizing diplexer coupling matrix, which is verified by our pilot experiments. For example, several popular improved DE even cannot detect the narrow valleys.

To the best of our knowledge, there are few works focusing on identifying the correct search direction for the targeted landscape. Therefore, the goal of the SADEC algorithm is to increase the probability of finding and preserving the correct search direction while maintaining its exploration ability. SADEC is based on DE and its design is described in Sections III-B and III-C.

B. Self-Adaptive Parameter Control Strategy

There are four key algorithmic parameters in DE, which are the population size (NP), the mutation strategy, the scaling factor (F), and the CR. The selection of them has a significant influence on the performance of DE for complex optimization problems [28], [29]. The mutation strategy and the scaling factor control the exploration of the decision space. In particular, the mutation strategy can be considered as the choice of the search direction, while the scaling factor can be considered as the step length. An example is the DE/rand/1 mutation (4). Selecting different kinds of mutation strategies and scaling factor leads to different capabilities of exploration. Besides, by increasing the size of the population, the exploration ability is promoted. As described above, the probability of finding the correct search direction is therefore decreased. According to (5), the crossover operator decides how many decision variables in expectation are changed in a population member. Thus, it decides to what extent that the visited search patterns (or search directions) can be changed/preserved.

A central question then becomes how to control these parameters so as to promote the probability of finding and preserving the correct search directions while maintaining the exploration ability. As described in Section III-A, there

are almost no guidelines for the landscapes of the targeted problem. Hence, empirical tests using various coupling matrix synthesis problems with different complexities are carried out and the following observations are obtained: 1) the inventor of DE suggests that the population size NP should be around $5 \times D$ to $10 \times D$ [16]. Our experiments show that when using the DE/rand/1 mutation with a reasonable scaling factor, NP = $5 \times D$ always provides enough exploration ability and 2) when using DE mutation strategies with higher exploration ability than DE/rand/1 (e.g., DE/rand/2 [16]), the probability of visiting the narrow valleys decreases. Given the settings of NP = $5 \times D$ and the DE/rand/1 mutation, the control of F and CR is discussed in the following.

Considering the characteristics of the targeted landscape, large F is needed to explore the decision space so as to get access to the narrow valleys. Small F is also needed to perform local exploitation in the narrow valley. Price *et al.* [16] suggest that F should not be smaller than 0.4, while a widely used parameter study Gämperle *et al.* [30] argue that the lower bound of F is problem dependent. Both studies suggest that if F is larger than 1.0, the convergence speed will decrease. Price *et al.* [16] and Gämperle *et al.* [30] recommend to use $F = 0.5$ and $F = 0.6$ as a default value, respectively. Considering above, SADEC uses the following method to decide the scaling factor:

$$F_{\text{temp}} = \text{norm}(0.5, 0.25)$$
$$F^i(t) = \begin{cases} 1, & \text{if } F_{\text{temp}} > 1 \\ 0.1, & \text{if } F_{\text{temp}} < 0.1 \\ F_{\text{temp}}, & \text{otherwise} \end{cases} \tag{7}$$

where norm(0.5, 0.25) is a Gaussian distributed random number with a mean of 0.5 and a standard deviation of 0.25.

It can be seen that: 1) because of the Gaussian distribution, there is about 68% probability, the generated F is between 0.25 and 0.75 (near the recommended default values). For about 27% probability, F is between 0.1 and 0.25 or between 0.75 and 1 (emphasizes exploration or exploitation in particular) and 2) for each candidate solution in each iteration, there is a separate F. In this way, different kinds of candidate designs have the opportunity to use various kinds of F (i.e., step size) in an appropriate range to either perform exploration or exploitation.

In terms of CR control strategy, various DE parameter studies show different recommendations [16], [30], [31]. Unfortunately, none of them works in our pilot tests using diplexer coupling matrix synthesis problems. In our empirical study, using various candidate solutions (x) and their mutant vectors (v) in the optimization process, a number of child candidates (u) are generated for a certain CR value. The number of successful crossovers, for which, u is better than x, can be observed. Two main observations include: 1) for different candidate solutions, there is not a universal workable CR value and the fit CR values can be very different and 2) in many cases, the workable CR value for a candidate solution spans in a narrow range (e.g., 0.4–0.5). This explains why a fixed setting rule of CR cannot work for the targeted problem. Therefore, a possible way is to explore random CR values and inherit the workable ones, which is shown as follows:

$$\text{CR}_{\text{temp}} = 0.1 + \text{rand}_1 \times 0.8$$
$$\text{CR}^i(t) = \begin{cases} \text{CR}_{\text{temp}}, & \text{if } \text{rand}_2 < 0.1 \\ \text{CR}^i(t-1), & \text{otherwise} \end{cases} \tag{8}$$

where rand is a uniformly distributed random number between 0 and 1. $\text{CR}(1) = 0.9$, which is based on the suggested default value in [16].

It can be seen that for 10% probability, CR can be any value between 0.1 and 0.9 (the possible range suggested by [16]); Otherwise, CR is inherited from the last iteration. Note that each candidate solution in the optimization process has its own CR value. Pilot experiments show that there is a considerable probability that a feasible CR for a certain candidate solution is sampled and inherited in the optimization process. Comparisons with several widely used self-adaptive setting rules (see [32]) show that this control method has the highest success rate.

C. Self-Adaptive Multipopulation Search Framework

Despite employing the above self-adaptive parameter control mechanism, obtaining the appropriate F and CR values cannot be guaranteed. Sometimes, the optimization converges to narrow valleys that only contain local optima (such as point B in Fig. 1). In almost all of the local optima that we have encountered, some resonance happens in undesired frequency ranges, while the others are correct. Hence, a new operator, called self-adaptive return operator, is activated when the optimization is judged to be trapped in local optima, which can often be observed in earlier iterations if it happens. The judgment of being trapped in local optima is based on two conditions: 1) the maximum standard deviation of decision variables in the current population is smaller than a predefined threshold δ and 2) the number of reflection zeros in any passband is incorrect. Using the return operator, the optimization returns to the original initial population, and the F and CR will be resampled based on (7) and (8) and the optimization process will restart. The effectiveness of this operator is shown by various test cases, and an example is shown in Section IV-B.

Uhm *et al.* [7] shows that the choice of initial population has an effect on the final result for coupling matrix synthesis problems. Our pilot experiments show a similar observation that some initial populations have a higher probability to obtain the desired global optimum than others using the same process in Section III-B. Hence, a multipopulation framework is proposed to increase the success rate.

Two populations are used. For one of them (P), the initialization is based on random sampling. The initialization of the other one ($\bar{P}$) is the opposite population of P, which is composed by

$$\bar{x}^i(1) = a + b - x^i(1) \tag{9}$$

where $x^i(1)$ is the ith candidate solution in initial P, $\bar{x}^i(1)$ is the corresponding candidate solution in initial $\bar{P}$, and $[a, b]^d$ is the search range. Experiments show that in many cases, if the optimization is not successful when using P as the initial

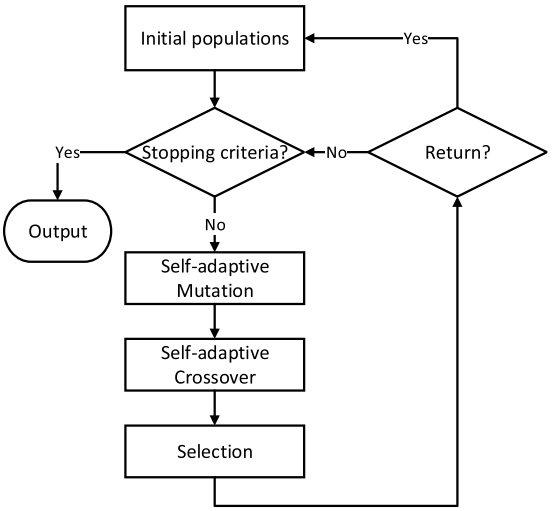

Fig. 2. Flow diagram of SADEC.

population, using $\bar{P}$ as the initial population has much larger success rate than using another randomly sampled population. This is understandable because $\bar{P}$ is often the best complement of P, covering search patterns that do not exist in P as much as possible.

D. General Framework of the SADEC Algorithm

The flow diagram of the SADEC algorithm is shown in Fig. 2, which consists the following steps.

- *Step 1:* Initialize P and $\bar{P}$ using the method in Section III-C. Initialize NP to be $5 \times D$. Initialize CR to be 0.9 for the crossover of the first iteration.
- *Step 2:* Check if the stopping criteria (e.g., a certain number of iterations) are met. If yes, output the result; otherwise, go to Step 3.
- *Step 3:* Apply the DE/rand/1 mutation (4) on P and $\bar{P}$ to generate mutant vectors V_p and $V_{\bar{p}}$. Use (7) to generate F values for the composing of each mutant vector.
- *Step 4:* Apply the crossover operator (5) on V_p and $V_{\bar{p}}$ to generate U_p and $U_{\bar{p}}$. If it is in the first iteration, CR $= 0.9$; otherwise, use (8) to generate CR for each crossover.
- *Step 5:* Apply the selection operator (6) to generate P and $\bar{P}$ for the next iteration.
- *Step 6:* Check if the return criteria for P or $\bar{P}$ are met. If yes, return to the corresponding initial population(s) and go to Step 2; otherwise, go to Step 3.

The only user defined algorithmic parameter in SADEC is δ when judging whether the population is trapped in a local optimum or not, which is the threshold of the maximum standard deviation of the decision variables in the current population. This threshold should be small enough making sure that the difference between the members of the current population is small, indicating that convergence happens. Clearly, this parameter is not sensitive if it is small enough, and the worst case is wasting function evaluations when the search stucks in a narrow valley that only contains a local optimum. Considering the search range of (normalized) coupling matrix optimization problems, which is often around $[-1, 1]$, a recommended setting is $\delta = 0.01$.

IV. Numerical Results and Comparisons

SADEC has been tested by coupling matrix synthesis problems of seven real-world all-resonator-based diplexers. SADEC obtains high-quality results with very high success rate to all of them. In this section, two examples are used to demonstrate different operators in SADEC. To the best of our knowledge, there are no general global optimization-based methods to solve them. The two diplexers have Chebyshev response, but SADEC is applicable to any response (e.g., Butterworth response) that can be generated by a coupling matrix. In both examples, the sum of normalized constraint violations is set as the cost function to be minimized. Because we are working with normalized values, practical diplexers can in principle be made at any frequency with any type of resonator [1]. Hence, we only concentrate on the normalized coupling matrix in the following.

For both examples, 20 runs are carried out for SADEC, standard DE, and PSO and the results are compared statistically. DE and PSO are the state-of-the-art global optimization methods, which have both strong global exploration and local exploitation ability. The stopping criterion for SADEC is that the maximum number of activating the return operator is 3 and the maximum number of iterations after each activation (if there is) is 1000. If the return operator is not activated, the maximum number of iterations is 1000. The stopping criterion for DE and PSO is also 1000 iterations. In all the runs for the three methods, the convergence happens before 1000, either stucks in a local optimum or obtains a successful result.

For the parameter setting of standard DE, the population size is the same as SADEC, the same DE/rand/1 mutation is used. As suggested by [16] and [33], $F = 0.5$, CR $= 0.9$ are used. PSO is implemented using the MATLAB Global Optimization Toolbox. The star topology is used. As suggested by [34], the cognitive coefficient and the social coefficient are both set to 2. According to [35], when the swarm size is larger than 50, PSO is not sensitive to the size of the population. Similar to DE, to improve the probability of finding the correct search direction, larger swarm size should not be used. Hence, the swarm size is set to 50. There are various methods to set the inertia weight. Our experiments show that using a constant inertia weight of 0.4 shows the best performance, which is used for comparison.

The examples are run on a PC with Intel 3.5-GHz Core (TM) i7 CPU and 8-GB RAM under Windows operating system. Since each function evaluation costs around 1 s, computational time is not a problem. Each SADEC run often costs about 40 min to 1 h, while each DE and PSO runs often costs about 20 min. In the SADEC optimization, the number of cost function calls, for example, 1 is around 1660 and that, for example, 2 is around 2870. In each cost function evaluation, 4000 frequencies are swept.

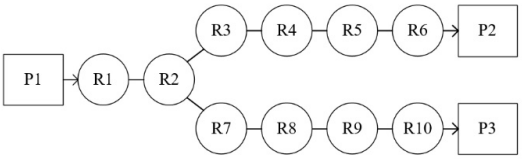

Fig. 3. Topology of example 1.

A. Example 1

The first example is a 10-resonator diplexer with a symmetrical Chebyshev response [36] (Fig. 3), which is a moderate test case among all the problems. This is a novel all-resonator-based diplexer topology that eliminates the need of additional common junction such as T-junction or power splitter. It is especially suitable for applications that need reduced size and volume of the circuit. A full description is in [36]. Due to the symmetry of the response and topology, the total number of variables in the coupling matrix is reduced to 9 [36]. The external quality factors can be straightforwardly calculated, which are $q_{e1} = 1.943$ and $q_{e2} = q_{e3} = 3.886$. The ranges of the design variables are in Table I. The design variables are the coupling matrix elements m_{ij} defined in (2). It can be seen that the search range is decided without any careful selection and no additional information is provided to SADEC. The design specifications over the normalized frequency are: two passbands (PB_1 and PB_2) are with the same bandwidth of 0.5 centered at -0.75 and 0.75 and the $\max(|S_{11}|)$ within the passband should be at least less than -20 dB. The normalized stopbands for channel 1 (PB_{1L} and PB_{1R}) are from -2 to 0.25 and from 1.25 to 2, where the $\max(|S_{21}|)$ should be less than -20 dB. The normalized stopbands for channel 2 (PB_{2L} and PB_{2R}) are from -2 to -1.25 and from -0.25 to 2, where the $\max(|S_{31}|)$ should be less than -20 dB. The design specifications are

$$\begin{aligned} \text{PB}_1 &\le -20 \text{ dB} \\ \text{PB}_2 &\le -20 \text{ dB} \\ \text{PB}_{1L} &\le -20 \text{ dB} \\ \text{PB}_{1R} &\le -20 \text{ dB} \\ \text{PB}_{2L} &\le -20 \text{ dB} \\ \text{PB}_{2R} &\le -20 \text{ dB} \end{aligned} \tag{10}$$

where

$$\begin{aligned} \text{PB}_1 &= \max(|S_{11}|), 0.5 \text{ to } 1 \\ \text{PB}_2 &= \max(|S_{11}|), -1 \text{ to } -0.5 \\ \text{PB}_{1L} &= \max(|S_{21}|), -2 \text{ to } 0.25 \\ \text{PB}_{1R} &= \max(|S_{21}|), 1.25 \text{ to } 2 \\ \text{PB}_{2L} &= \max(|S_{31}|), -2 \text{ to } -0.75 \\ \text{PB}_{2R} &= \max(|S_{31}|), -0.25 \text{ to } 2 \end{aligned} \tag{11}$$

where the numbers in (11) are normalized frequencies.

TABLE I
RANGES OF THE NINE DECISION VARIABLES FOR EXAMPLE 1

$Variables$	m_{12}	m_{23}	m_{34}	m_{45}	m_{56}
Lower bound	0	0	0	0	0
Upper bound	1	1	1	1	1
$Variables$	m_{33}	m_{44}	m_{55}	m_{66}	
Lower bound	0	0	0	0	
Upper bound	1	1	1	1	

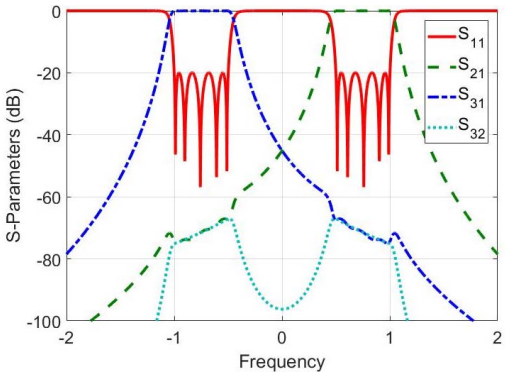

Fig. 4. Example 1: response of a typical optimized solution by SADEC.

TABLE II
TYPICAL OPTIMAL RESULT FOR EXAMPLE 1

$Variables$	m_{12}	m_{23}	m_{34}	m_{45}	m_{56}
Values	0.8204	0.2856	0.1625	0.1598	0.2170
$Variables$	m_{33}	m_{44}	m_{55}	m_{66}	
Values	0.7004	0.7442	0.7478	0.7487	

The cost function is defined as

$$\begin{aligned} f_1 = &\frac{\max(\text{PB}_1 - (-20), 0)}{M_{\text{PB}_1}} + \frac{\max(\text{PB}_2 - (-20), 0)}{M_{\text{PB}_2}} \\ &+ \frac{\max(\text{PB}_{1L} - (-20), 0)}{M_{\text{PB}_{1L}}} + \frac{\max(\text{PB}_{1R} - (-20), 0)}{M_{\text{PB}_{1R}}} \\ &+ \frac{\max(\text{PB}_{2L} - (-20), 0)}{M_{\text{PB}_{2L}}} + \frac{\max(\text{PB}_{2R} - (-20), 0)}{M_{\text{PB}_{2R}}} \end{aligned} \tag{12}$$

where M_{PB_1} is the $\max\{\max(\text{PB}_1 - (-20), 0)\}$ so far (i.e., the maximum violation of the $\text{PB}_1 \le -20$-dB constraint, found so far), so do the others.

A typical response of SADEC is shown in Fig. 4, and the corresponding optimal design variables are shown in Table II. Other normalized coupling coefficients are: $m_{27} = m_{23}$, $m_{78} = m_{34}$, $m_{89} = m_{45}$, $m_{9,10} = m_{56}$, $m_{77} = -m_{33}$, $m_{88} = -m_{44}$, $m_{99} = -m_{55}$, and $m_{10,10} = -m_{66}$. Plugging in the optimal values to (2) and then to (1), the response can be obtained. The average optimized responses of SADEC, standard DE, and PSO are shown in Table III. It can be seen that SADEC obtains successful results and is much better than DE and PSO in terms of optimization quality for this example.

The most important criterion for comparison is the success rate. In a diplexer design flow, the coupling matrix synthesis provides an initial design for 3-D EM simulation-driven design

TABLE III
OPTIMIZED RESULTS USING DIFFERENT METHODS FOR EXAMPLE 1 (AVERAGE OF 20 RUNS, IN DECIBEL)

Methods	PB_1	PB_2	PB_{1L}	PB_{1R}	PB_{2L}	PB_{2R}
SADEC	–19.92	–19.92	–27.64	–23.15	–23.36	–27.40
DE	–14.97	–14.97	–27.23	–20.22	–23.36	–27.40
PSO	–5.29	–5.25	–20.00	–19.97	–19.98	–20.00

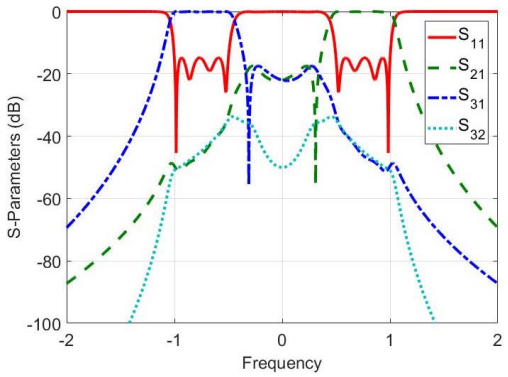

Fig. 5. Local optimum (example 1).

optimization, rather than the final design. Hence, we define a successful result based on the following rules: 1) the reflection zeros are located in proper frequency ranges and the number is correct. A poor example is shown in Fig. 5. We consider that it is a local optimum, because performing various kinds of local optimization (e.g., sequential quadratic programming) from this starting point cannot find a better solution. When it comes to 3-D EM simulation-driven local optimization, experiments show that using such a starting point often cannot obtain a successful final design and 2) the S-parameter design specifications are (almost) satisfied.

Using the above rules, the success rate of SADEC is 20/20, while those for DE and PSO are 4/20 and 1/20, respectively. Most DE and PSO runs obtain solutions like Fig. 5 (like point B in Fig. 1). For SADEC, in 17/20 runs, the return operator is not activated to either P or $\bar{P}$, which means that successful results are obtained directly using the self-adaptive parameter control strategy starting from both P and $\bar{P}$. In the other three runs, the return operator is only activated for once and successful results are obtained. This verifies the considerable improvement of the capacity of finding and preserving correct search directions compared to standard DE, thanks to the algorithm parameter control strategy in Section III-B.

B. Example 2

The second example is a 12-resonator diplexer with a cross-coupling topology shown in [18] (Fig. 6). This topology allows the design of diplexers with sharp rejection in the guard band and is especially suitable for applications that require a reduced guard bandwidth. A full description is in [18]. A cross coupling between resonators 2 and 5 is introduced in a quadruplet to provide a pair of transmission zeros for both channels. Using the symmetry characteristics of the diplexer, the total number of variables is reduced to 12 [18]. The ranges

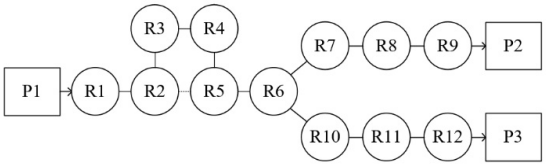

Fig. 6. Topology of example 2.

of design variables are in Table IV. Again, the search range is decided without any careful selection and no additional information is provided to SADEC. The design specifications over the normalized frequency are: two passbands (PB_1 and PB_2) are with the same bandwidth of 0.5 centered at -0.75 and 0.75 and the $\max(|S_{11}|)$ within the passband should be at least less than -20 dB. The constraints for the middle guard bands (PB_{1M} and PB_{2M}) (-0.3 to 0.3) of channels 1 and 2 are that $\max(|S_{21}|)$ and $\max(|S_{31}|)$ should be less than -40 dB due to the introduction of transmission zeros. The $\max(|S_{21}|)$ for the right stopband of channel 1 (PB_{1R}) (1.2 to 2) and $\max(|S_{31}|)$ for the left stopband of channel 2 (PB_{2L}) (-2 to -1.2) should be less than -20 dB. Therefore, the optimization problem is formulated as

$$\begin{aligned} \text{PB}_1 &\le -20 \text{ dB} \\ \text{PB}_2 &\le -20 \text{ dB} \\ \text{PB}_{1M} &\le -40 \text{ dB} \\ \text{PB}_{2M} &\le -40 \text{ dB} \\ \text{PB}_{1R} &\le -20 \text{ dB} \\ \text{PB}_{2L} &\le -20 \text{ dB} \end{aligned} \tag{13}$$

where

$$\begin{aligned} \text{PB}_1 &= \max(|S_{11}|), 0.5 \text{ to } 1 \\ \text{PB}_2 &= \max(|S_{11}|), -1 \text{ to } -0.5 \\ \text{PB}_{1M} &= \max(|S_{21}|), -0.3 \text{ to } 0.3 \\ \text{PB}_{2M} &= \max(|S_{31}|), -0.3 \text{ to } 0.3 \\ \text{PB}_{1R} &= \max(|S_{21}|), 1.2 \text{ to } 2 \\ \text{PB}_{2L} &= \max(|S_{31}|), -2 \text{ to } -1.2 \end{aligned} \tag{14}$$

where the numbers in (14) are normalized frequencies.

The cost function is defined as

$$\begin{aligned} f_2 = &\frac{\max(\text{PB}_1 - (-20), 0)}{M_{\text{PB}_1}} + \frac{\max(\text{PB}_2 - (-20), 0)}{M_{\text{PB}_2}} \\ &+ \frac{\max(\text{PB}_{1M} - (-40), 0)}{M_{\text{PB}_{1M}}} + \frac{\max(\text{PB}_{2M} - (-40), 0)}{M_{\text{PB}_{2M}}} \\ &+ \frac{\max(\text{PB}_{1R} - (-20), 0)}{M_{\text{PB}_{1R}}} + \frac{\max(\text{PB}_{2L} - (-20), 0)}{M_{\text{PB}_{2L}}} \end{aligned} \tag{15}$$

where M_{PB_1} is the $\max\{\max(\text{PB}_1 - (-20), 0)\}$ so far (i.e., the maximum violation of the $\text{PB}_1 \le -20$-dB constraint, found so far), so do the others.

A typical response of SADEC is shown in Fig. 7, and the corresponding optimal design variables are shown in Table V. Other normalized coupling coefficients are: $m_{6,10} = m_{67}$, $m_{10,11} = m_{78}$, $m_{11,12} = m_{89}$, $m_{10,10} = -m_{77}$, $m_{11,11} = -m_{88}$, and $m_{12,12} = -m_{99}$. The average optimized responses

TABLE IV
RANGES OF THE 12 DECISION VARIABLES FOR EXAMPLE 2

$Variables$	m_{12}	m_{23}	m_{34}	m_{45}	m_{56}	m_{67}
Lower bound	0	0	0	0	0	0
Upper bound	1	1	1	1	1	1
$Variables$	m_{78}	m_{89}	m_{77}	m_{88}	m_{99}	m_{25}
Lower bound	0	0	0	0	0	0
Upper bound	1	1	1	1	1	1

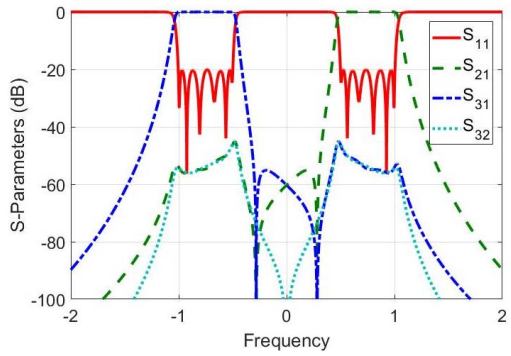

Fig. 7. Example 2: response of a typical optimized solution by SADEC.

TABLE V
TYPICAL OPTIMAL RESULT FOR EXAMPLE 2

$Variables$	m_{12}	m_{23}	m_{34}	m_{45}	m_{56}	m_{67}
Values	0.8278	0.3519	0.5786	0.2450	0.7609	0.2087
$Variables$	m_{78}	m_{89}	m_{77}	m_{88}	m_{99}	m_{25}
Values	0.1558	0.2142	0.7395	0.7495	0.7501	0.1955

TABLE VI
OPTIMIZED RESULTS USING DIFFERENT METHODS FOR EXAMPLE 2 (AVERAGE OF 20 RUNS, IN DECIBEL)

Methods	PB_1	PB_2	PB_{1M}	PB_{2M}	PB_{1R}	PB_{2L}
SADEC	–19.82	–19.83	–32.88	–46.92	–47.14	–32.61
DE	–9.05	–9.05	–26.41	–38.41	–38.39	–26.23
PSO	–3.19	–3.17	–19.94	–39.69	–39.71	–19.92

of SADEC, standard DE, and PSO are shown in Table VI. It can be seen that SADEC obtains successful results and is much better than DE and PSO in terms of optimization quality for this example.

In this example, the success rate of SADEC is 20/20, while those for DE and PSO are 0/20 and 0/20, respectively. In 11/20 runs, the return operator is not activated to either P or $\bar{P}$ in SADEC. Among these 11 runs, successful results are obtained from either P or $\bar{P}$ in 10 of them (only starting from P or $\bar{P}$ obtains successful results); for the other one run, successful results are obtained from both P and $\bar{P}$. This verifies that using two opposite populations, P and $\bar{P}$, in initialization establishes an effective complementation. Among the other 9 runs, the return operator is only activated for once in 7 of them; among 2/9 runs, the return operator is activated for twice and successful results are obtained. These nine runs verify the effectiveness of the return operator to avoid converging into a narrow valley that only contains local optima.

It is intuitive that with the increase of the number of decision variables, the valley that contains the global optimum is narrower and narrower with respect to the decision space. This causes any optimization algorithm, including SADEC, to have difficulty in detecting the narrow valley. We found that for coupling matrix synthesis problems with more than 25 design variables, the success rate of SADEC is low if using large search ranges only with the requirement of matching the topology (e.g., $[-1, 1]^{25}$). In such cases, the support from analytical methods that reasonably narrow down the search ranges is needed. Note that SADEC does not aim to replace the analytical methods; instead, it aims to provide a much stronger optimizer than the existing general purpose optimizers applied in hybrid analytical and optimization-based coupling matrix synthesis methods.

V. CONCLUSION

In this paper, the SADEC algorithm for diplexer coupling matrix synthesis has been proposed. SADEC aims at filling the gap that strong supporting information (e.g., high-quality starting points and narrow enough search ranges) from analytical methods is essential for the success of diplexer coupling matrix synthesis when employing available general purpose optimizers. SADEC focuses on proposing a stronger optimization mechanism especially for the targeted problem, which only requires weak, easy to obtain, or highly reduced supporting information in most cases. Experiments show that SADEC is able to obtain highly optimized coupling matrix solutions with very high success rate even without *ad hoc* supporting information for various diplexers. Much better solution quality and success rate are shown compared with the state-of-the-art global optimization methods, DE and PSO. These results are achieved by our self-adaptive parameter control strategy and self-adaptive multipopulation search framework. Future works include developing software tools using SADEC and coupling matrix synthesis for multiplexers.

ACKNOWLEDGMENT

The authors would like to thank Dr. X. Shang, University of Birmingham, Birmingham, U.K., for valuable discussions.

REFERENCES

[1] J.-S. G. Hong and M. J. Lancaster, *Microstrip Filters for RF/Microwave Applications*, vol. 167. Hoboken, NJ, USA: Wiley, 2004.
[2] J. W. Bandler, R. M. Biernacki, S. H. Chen, P. A. Grobelny, and R. H. Hemmers, "Space mapping technique for electromagnetic optimization," *IEEE Trans. Microw. Theory Techn.*, vol. 42, no. 12, pp. 2536–2544, Dec. 1994.
[3] B. Liu, H. Yang, and M. J. Lancaster, "Global optimization of microwave filters based on a surrogate model-assisted evolutionary algorithm," *IEEE Trans. Microw. Theory Techn.*, vol. 65, no. 6, pp. 1976–1985, Jun. 2017.
[4] A. Atia, A. Williams, and R. Newcomb, "Narrow-band multiple-coupled cavity synthesis," *IEEE Trans. Circuits Syst.*, vol. CAS-21, no. 5, pp. 649–655, Sep. 1974.
[5] R. J. Cameron, "General coupling matrix synthesis methods for Chebyshev filtering functions," *IEEE Trans. Microw. Theory Techn.*, vol. 47, no. 4, pp. 433–442, Apr. 1999.
[6] S. Tamiazzo and G. Macchiarella, "Synthesis of cross-coupled filters with frequency-dependent couplings," *IEEE Trans. Microw. Theory Techn.*, vol. 65, no. 3, pp. 775–782, Mar. 2017.

[7] M. Uhm, S. Nam, and J. Kim, "Synthesis of resonator filters with arbitrary topology using hybrid method," *IEEE Trans. Microw. Theory Techn.*, vol. 55, no. 10, pp. 2157–2167, Oct. 2007.

[8] G. L. Nicholson and M. J. Lancaster, "Coupling matrix synthesis of cross-coupled microwave filters using a hybrid optimisation algorithm," *IET Microw., Antennas Propag.*, vol. 3, no. 6, pp. 950–958, Sep. 2009.

[9] X. Shang, Y. Wang, G. Nicholson, and M. J. Lancaster, "Design of multiple-passband filters using coupling matrix optimisation," *IET Microw., Antennas Propag.*, vol. 6, no. 1, pp. 24–30, Jan. 2012.

[10] L. Szydlowski, A. Lamecki, and M. Mrozowski, "A novel coupling matrix synthesis technique for generalized Chebyshev filters with resonant source–load connection," *IEEE Trans. Microw. Theory Techn.*, vol. 61, no. 10, pp. 3568–3577, Oct. 2013.

[11] D. A. Tubail and T. F. Skaik, "Synthesis of coupled resonator-based multiplexers with generalised structures using coupling matrix optimisation," *Electron. Lett.*, vol. 51, no. 23, pp. 1891–1893, Nov. 2015.

[12] M. Mokhtaari, J. Bornemann, K. Rambabu, and S. Amari, "Coupling-matrix design of dual and triple passband filters," *IEEE Trans. Microw. Theory Techn.*, vol. 54, no. 11, pp. 3940–3946, Nov. 2006.

[13] A. Lamecki, P. Kozakowski, and M. Mrozowski, "Fast synthesis of coupled-resonator filters," *IEEE Microw. Wireless Compon. Lett.*, vol. 14, no. 4, pp. 174–176, Apr. 2004.

[14] W. A. Atia, K. A. Zaki, and A. E. Atia, "Synthesis of general topology multiple coupled resonator filters by optimization," in *IEEE MTT-S Int. Microw. Symp. Dig.*, vol. 2. Jun. 1998, pp. 821–824.

[15] W. Xia, "Diplexers and multiplexers design by using coupling matrix optimisation," Ph.D. dissertation, School Electron., Elect. Syst. Eng., Univ. Birmingham, Birmingham, U.K., 2015.

[16] K. Price, R. Storn, and J. Lampinen, *Differential Evolution: A Practical Approach to Global Optimization*. New York, NY, USA: Springer-Verlag, 2005.

[17] J. Kennedy, "Particle swarm optimization," in *Encyclopedia of Machine Learning*. Boston, MA, USA: Springer, 2011, pp. 760–766.

[18] X. Shang, Y. Wang, W. Xia, and M. J. Lancaster, "Novel multiplexer topologies based on all-resonator structures," *IEEE Trans. Microw. Theory Techn.*, vol. 61, no. 11, pp. 3838–3845, Nov. 2013.

[19] J. C. Lagarias, J. A. Reeds, M. H. Wright, and P. E. Wright, "Convergence properties of the Nelder–Mead simplex method in low dimensions," *SIAM J. Optim.*, vol. 9, no. 1, pp. 112–147, 1998.

[20] P. T. Boggs and J. W. Tolle, "Sequential quadratic programming," *Acta Numer.*, vol. 4, pp. 1–51, Jan. 1995.

[21] Ł. Januszkiewicz, P. Di Barba, and S. Hausman, "Field-based optimal placement of antennas for body-worn wireless sensors," *Sensors*, vol. 16, no. 5, p. 713, May 2016.

[22] Ł. Januszkiewicz, P. Di Barba, and S. Hausman, "Automated identification of human-body model parameters," *Int. J. Appl. Electromagn. Mech.*, vol. 51, no. s1, pp. S41–S47, Apr. 2016.

[23] U. Singh, H. Kumar, and T. S. Kamal, "Design of Yagi-Uda antenna using biogeography based optimization," *IET Microw., Antennas Propag.*, vol. 58, no. 10, pp. 3375–3379, Oct. 2010.

[24] B. Liu, D. Zhao, P. Reynaert, and G. G. E. Gielen, "GASPAD: A general and efficient mm-wave integrated circuit synthesis method based on surrogate model assisted evolutionary algorithm," *IEEE Trans. Comput.-Aided Design Integr.*, vol. 33, no. 2, pp. 169–182, Feb. 2014.

[25] M. Jamil and X.-S. Yang, "A literature survey of benchmark functions for global optimisation problems," *Int. J. Math. Model. Numer. Optim.*, vol. 4, no. 2, pp. 150–194, Feb. 2013.

[26] E. Mezura-Montes, J. Velázquez-Reyes, and C. A. C. Coello, "A comparative study of differential evolution variants for global optimization," in *Proc. 8th Annu. Conf. Genetic Evol. Comput.*, 2006, pp. 485–492.

[27] S. Das and P. N. Suganthan, "Differential evolution: A survey of the state-of-the-art," *IEEE Trans. Evol. Comput.*, vol. 15, no. 1, pp. 4–31, Feb. 2011.

[28] Y. Wang, Z. Cai, and Q. Zhang, "Differential evolution with composite trial vector generation strategies and control parameters," *IEEE Trans. Evol. Comput.*, vol. 15, no. 1, pp. 55–66, Feb. 2011.

[29] J. Brest, S. Greiner, B. Boskovic, M. Mernik, and V. Zumer, "Self-adapting control parameters in differential evolution: A comparative study on numerical benchmark problems," *IEEE Trans. Evol. Comput.*, vol. 10, no. 6, pp. 646–657, Dec. 2006.

[30] R. Gämperle, S. D. Müller, and P. Koumoutsakos, "A parameter study for differential evolution," in *Advances in Intelligent Systems, Fuzzy Systems, Evolutionary Computation*. New York, NY, USA: Springer, 2002, pp. 293–298.

[31] J. Ronkkonen, S. Kukkonen, and K. V. Price, "Real-parameter optimization with differential evolution," in *Proc. IEEE Congr. Evol. Comput.*, vol. 1. Sep. 2005, pp. 506–513.

[32] A. K. Qin, V. L. Huang, and P. N. Suganthan, "Differential evolution algorithm with strategy adaptation for global numerical optimization," *IEEE Trans. Evol. Comput.*, vol. 13, no. 2, pp. 1785–1791, Apr. 2005.

[33] J. Vesterstrom and R. Thomsen, "A comparative study of differential evolution, particle swarm optimization, and evolutionary algorithms on numerical benchmark problems," in *Proc. Congr. Evol. Comput.*, vol. 2. Jun. 2004, pp. 1980–1987.

[34] J. Kenndy and R. Eberhart, "Particle swarm optimization," in *Proc. Int. Conf. Neural Netw.*, vol. 4. Nov./Dec. 1995, pp. 1942–1948.

[35] R. C. Eberhart, Y. Shi, and J. Kennedy, *Swarm Intelligence*. Amsterdam, The Netherlands: Elsevier, 2001.

[36] W. Xia, X. Shang, and M. J. Lancaster, "Responses comparisons for coupled-resonator based diplexers," in *Proc. 3rd Annu. Seminar Passive RF Microw. Compon.*, Mar. 2012, pp. 67–75.

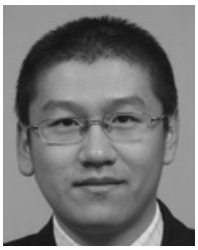

Bo Liu (M'15–SM'17) received the B.S. degree from Tsinghua University, Beijing, China, in 2008, and the Ph.D. degree from the MICAS Laboratories, University of Leuven, Leuven, Belgium, in 2012.

From 2012 to 2013, he was a Humboldt Research Fellow and was with the Technical University of Dortmund, Dortmund, Germany. In 2013, he was a Lecturer with Wrexham Glyndwr University, Wrexham, U.K., where he was a Reader in computer-aided design in 2016. He is currently an Honorary Fellow with the University of Birmingham, Birmingham, U.K. He has authored or co-authored 1 book and more than 40 papers in international journals, edited books, and conference proceedings. His current research interests include the design automation methodologies of analog/RF integrated circuits, microwave devices, MEMS, evolutionary computation, and machine learning.

Hao Yang was born in Wuhan, China, in 1991. He received the B.Eng. degree in electronic and electrical engineering from the University of Birmingham, Birmingham, U.K., in 2014, and the B.Eng. degree in electronics and information engineering from the Huazhong University of Science and Technology, Wuhan, China, in 2014. He is currently pursuing the Ph.D. degree in electronic and electrical engineering at the University of Birmingham.

His current research interests include terahertz frequency filters and mutiplexers.

Michael J. Lancaster (SM'04) was born in West Yorkshire, U.K., in 1958. He received the bachelor's degree in physics and Ph.D. degree with a focus on nonlinear underwater acoustics from Bath University, Bath, U.K., in 1980 and 1984, respectively.

He joined the Surface Acoustic Wave (SAW) Group, Department of Engineering Science, Oxford University, Oxford, U.K., as a Research Fellow. He was involved in the design of new novel SAW devices, including RF filters and filter banks. In 1987, he was a Lecturer of electromagnetic theory and microwave engineering with the Department of Electronic and Electrical Engineering, University of Birmingham, Birmingham, U.K., where he was focused on the study of the science and applications of high-temperature superconductors, particularly in microwave frequencies. He was the Head of the Department of Electronic, Electrical and Systems Engineering in 2003. He has authored 2 books and over 190 papers in refereed journals. His current research interests include microwave filters and antennas, as well as the high-frequency properties and the applications of a number of novel and diverse materials, including micromachining as applied to terahertz communications devices and systems.

Prof. Lancaster is a Fellow of the IET and the U.K. Institute of Physics. He is a Chartered Engineer and Chartered Physicist. He has served on the IEEE MTT-S IMS Technical Committee.